



Simultaneous decolorization of binary mixture of blue disperse and yellow basic dyes by electrocoagulation

İ. Ayhan Şengil^{a,*}, Abdil Özdemir^b

^aEngineering Faculty, Department of Environmental Engineering, Sakarya University, 54100 Sakarya, Turkey
Tel. +90 264 2955454; Fax: +90 264 2955601; email: asengil@sakarya.edu.tr

^bDepartment of Chemistry, Science & Arts Faculty, Sakarya University, 54100 Sakarya, Turkey

Received 25 September 2011; Accepted 5 March 2012

ABSTRACT

In this paper, electrocoagulation (EC) has been used for the removal of color from solution containing a disperse dye (Disperse blue 56) and a basic dye (Basic Yellow 28) in the same solution. Iron electrodes were arranged in a monopolar fashion. In the EC of the dye mixture, the effects of the supporting electrolyte, initial pH, electrolysis time, and current density were examined. The results indicated that the majority of the aforementioned dyes in the synthetic wastewater were effectively removed when iron electrodes were used as a sacrificial anode. The amount of dye removed was found by the application of the first derivative spectrophotometric method to the synthetic dye mixtures. In the presence of both dye molecules, the optimum pH was found to be 7, optimum NaCl concentration was $3,000 \text{ mg L}^{-1}$, and optimum current density was 10.89 mA cm^{-2} . The experimental data were fit to a variety of isotherm models to determine the characteristics of the EC process. The results indicated that the model provided the best fit for the removal of dye mixture.

Keywords: Disperse blue 56; Basic yellow 28; Electrocoagulation; Derivative spectrophotometry

1. Introduction

The textile industry consumes considerable amount of water during dyeing and finishing operations. A typical textile effluent contains various types of dye molecules and might have fluctuating properties due to varying dyeing activities [1]. A dye-containing effluent is toxic to the environment since dyes are stable compounds, have low biodegradability, and can be carcinogenic. It is estimated that 1–15% of the dye is lost during dyeing and finishing processes and is released into wastewaters. The textile industry utilizes about 10,000 dyes and pigments [2]. Dye bath effluents impart color to

receiving streams and affect their esthetic value. The color blocks the penetration of sunlight into waters, retards photosynthesis, inhibits the growth of aquatic biota, and interferes with gas solubility in water bodies. Furthermore, dye effluents contain chemicals, that are toxic, carcinogenic, mutagenic, or teratogenic to various microbiological, fish species [3]. There are many processes to remove dyes from colored effluents such as adsorption [4–8], precipitation [9], chemical–biological degradation [10], photodegradation [11,12], biodegradation [13,14], chemical coagulation [15,16], Fenton oxidation [17], combined coagulation/flocculation and adsorption [18], and combination of coagulation–flocculation and nanofiltration [19]. EC as an electrochemical method was developed to overcome the drawbacks of

*Corresponding author.

conventional decolorization technologies. EC techniques are more effective than the others in decolorizing textile effluents. The EC process provides a simple, reliable and cost-effective method for the treatment of wastewater without the need for any additional chemicals, and thus avoiding secondary pollution. This process also reduces the amount of sludge, that needs to be disposed [20–24]. The main advantages of EC over other conventional techniques, such as chemical coagulation and adsorption, are the *in situ* delivery of reactive agents, no generation of secondary pollution, and compact equipment [23]. Many studies on the decolorization of textile dyes by the EC process focus on one dye class, e.g. Reactive Black 5 [20], Reactive Red 141 [25], Acid Red 14 [26,27], Reactive Red 124 [21], Acid Orange II [28], Bomaplex Red CR-L [29], Orange II [3,30], Levafix Orange E3 GA [31], Basic Red 46 [2], Green dye 50 [32], Direct [33], Acid Blue 9 [34], Direct Red 23 [35], Reactive Blue 140 and Disperse red 1 [23], Suncion Blue P-3R, Suncion Yellow H-E4RN, Suncron Blue RD-400, and Suncron Yellow 3GE-200 [36], Reactive Red (RR; with a confidential color index (CI) number), Reactive Yellow145, Reactive Blue 221 [37], Terasil yellow 4G, Red terasil 343, Blue terasil 3R02, Red S3B 195, Yellow SPD, and Blue Ridge Fiber Solutions [38].

UV-vis spectrometers are used to calculate the concentrations of dyes, which are based on the measurement at a wavelength corresponding to maximum absorbance of the dye. When more than one dye was

analyzed in a mixture, their spectra will most probably overlap in a certain wavelength region. Chemometric and graphical calibration techniques in spectral analysis can be used to solve this problem without any separation procedure before the determination step [39]. In this study, due to the spectral overlap, graphical solution was applied to determine the remaining amount of dye in the solution. The method utilized to calculate the amount of dye in the solution is a derivative spectrophotometric method. In this study, a first-order derivative method was developed and validated for the determination of the remaining dyes in solution. The method is based on the computation of calibration equations for both dyes and their application to samples.

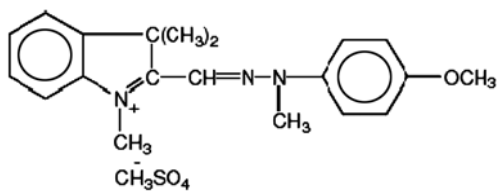
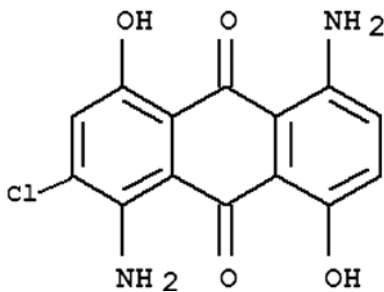
The objective of the present study was to investigate the simultaneous removal of Disperse blue 56 (DB56) and Basic yellow 28 (BY28) from aqueous solution via EC using iron as an electrode material. The effects of several parameters including initial pH, current density, initial dye concentration, and electrolysis time were investigated to measure the dyes' removal efficiency of EC process.

2. Materials and methods

2.1. Materials

The dyes used in the experiments were DB56 and BY28. The structures of dyes are shown in Table 1. DB56 and BY28 were obtained from Aldrich Chemical

Table 1
Studied textile dyes and name abbreviations used in this study

Code	Structural formulae	λ_{\max} (nm)	Commercial textile name
BY28		400	Sandocryl Gold Yellow
DB56		559	Disperse blue 56

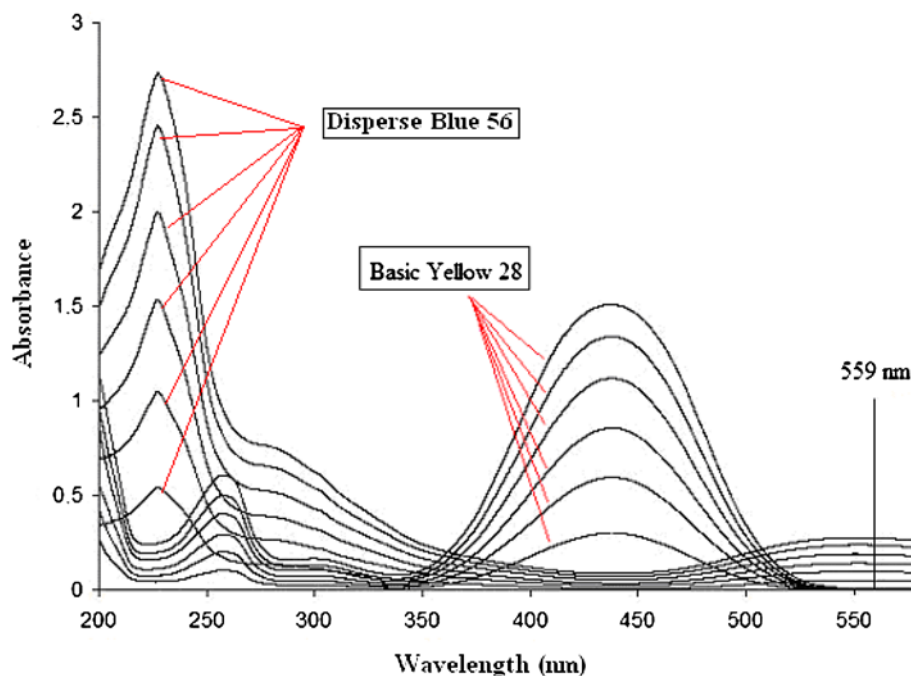


Fig. 1. Absorption spectra of DB56 and BY28 in different concentrations.

Company. In order to measure the dye concentrations, the solutions were analyzed by UV–vis spectrometer (Shimadzu UV–vis 160) measuring the full absorption spectrum of mixtures in the range of 200–800 nm (Fig. 1). Data treatments, regressions, and statistical analysis were performed by using the EXCEL software. The calibration procedure was carried out by using 14 calibration standards prepared using different concentrations of each dye. DB56 and BY28 concentrations were varied between 100 and 400 mg/L.

2.2. Design and method

The EC unit consists of an electrochemical reactor, a D.C. power supply, and iron electrodes. The iron cathode and iron anode consist of pieces of iron sheet separated by a space of 2.2 cm and dipped in wastewater. The electrodes were placed in 700 mL aqueous dye solutions in a 1,000 mL plexiglass electrolytic reactor. There were two electrodes connected in the electrochemical reactor, each one with dimensions of $9 \times 5 \times 0.2$ cm. The submerged surface area of the electrode plates was 91 cm^2 . The batch experimental setup is schematically shown in Fig. 2.

During the EC process proper mixing of the synthetic solution was provided by a stirrer. The stirrer was used in an electrochemical cell to maintain an unchanged composition and to avoid the association of the flocs in the solution. The electrodes were sanded and washed with dilute HCl before each experiment. The experiments were conducted at a

temperature of around 25°C . The dye solution was prepared by dissolving the dyes in distilled water. The conductivity of the solution was increased and adjusted to different values by the addition of NaCl. The pH of the solution was adjusted to a desirable value by adding HCl and NaOH solutions. At the beginning of a run the desired concentration of the dye in aqueous solution was fed into the reactor. The iron electrodes were placed into the reactor. The reaction was timed, starting when the D.C. power supply was switched on. Iron salts produce electrode passivation which causes a 50% increase in treatment time and power requirements. One of the greatest operational issues with EC is the electrode passivation. The samples were periodically taken from the reactor. The particulates of colloidal ferric oxyhydroxides gave a yellow-brown color into the solution after EC. The sedimentation was filtered with normal filter paper.

In order to calculate the dye concentrations, the maximum adsorption (λ_{max}) wavelength of dyes was determined by measuring their absorbance spectra (Fig. 1, Table 1). The calculation of the color removal efficiency after the EC treatment was performed using the following formula:

$$\text{CR (\%)} = \frac{C_0 - C}{C_0} \times 100 \quad (1)$$

where C_0 and C are the concentrations of the dye before and after EC in mg L^{-1} , respectively.

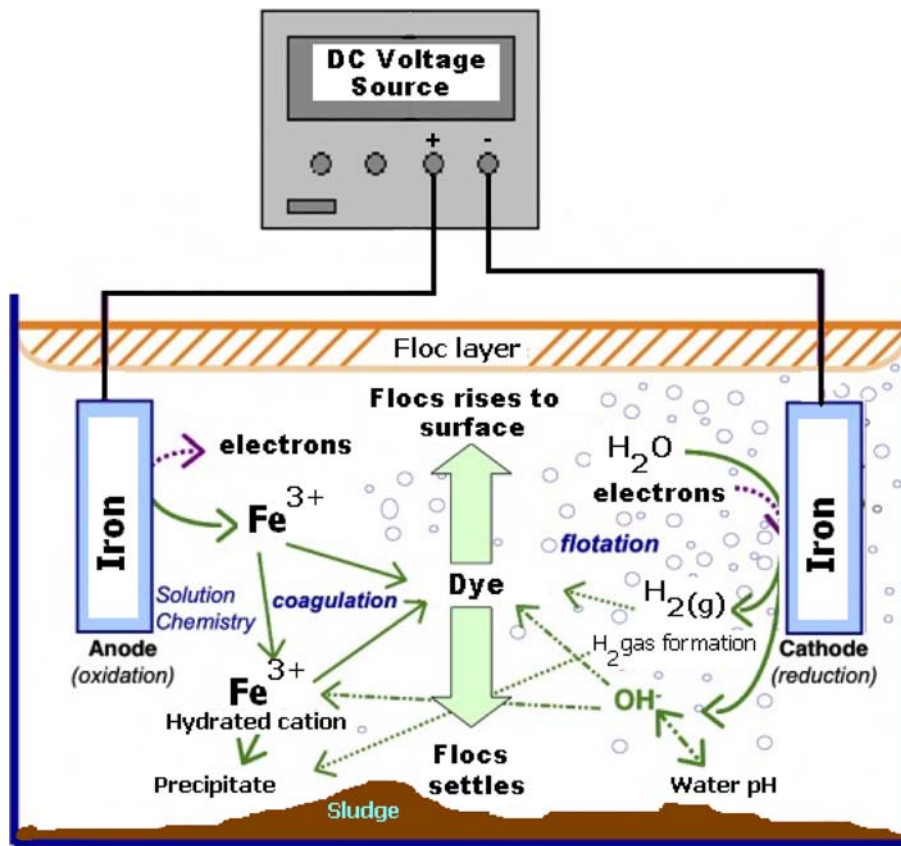


Fig. 2. Schematic representation of the EC process.

3. Results and discussion

The first derivative of the spectra was calculated by $\Delta\lambda=5\text{ nm}$ intervals and the resulting spectra are shown in Fig. 3. After derivation of the absorption spectra of compounds, zero crossing points were determined to establish two different calibration equations. For each compound, a graph was plotted by using concentration vs. absorption values. The amounts of DB56 and BY28 in the binary mixture were found to be proportional to the signals and statistical parameters of their calibration equations are summarized in Table 2. The validity of the calibrating method was tested by preparing various binary mixtures containing 0–100 mg/L DB56 and BY28 in water. The mean recoveries and the relative standard deviations (RSDs) were calculated and their results are given in Table 3. The RSD was used to express the precision of experiments. The following equation was used to calculate the RSD values of results.

$$\text{RSD} = \frac{\text{SD}}{\bar{x}} 100 \quad (2)$$

3.1. Effect of initial pH on the efficiency of color removal

It has been established that the influent pH is an important parameter influencing the performance of the EC process. The kinetics of Fe^{2+} conversion to Fe^{3+} are strongly affected by the pH; the surface charge of the coagulating particle also varies with the pH [20]. The variation in the efficiency of color removal of the dyes was studied in the pH range of 2–10, and the results are shown in Fig. 4. The maximum removals of DB56 and BY28 were 94.7% at pH 2–4 and 99.9% at pH 6–10, respectively. The total removal rate of the dyes was 91% at pH 6–10

If iron electrodes are used, the generated $\text{Fe}_{(\text{aq})}^{2+}$ ions will immediately undergo further spontaneous reactions to produce corresponding hydroxides and/or polyhydroxides. The $\text{Fe}(\text{II})$ ions are the common ions that are generated during the dissolution of iron. In contrast, OH^- ions are produced at the cathode. By mixing the solution, hydroxide species are produced which cause the removal of matrices (dyes and cations) by adsorption and coprecipitation. In the oxygenated water and at lower pH, Fe^{2+} is easily converted to Fe^{3+} . The $\text{Fe}(\text{OH})_n(\text{s})$ formed remains in

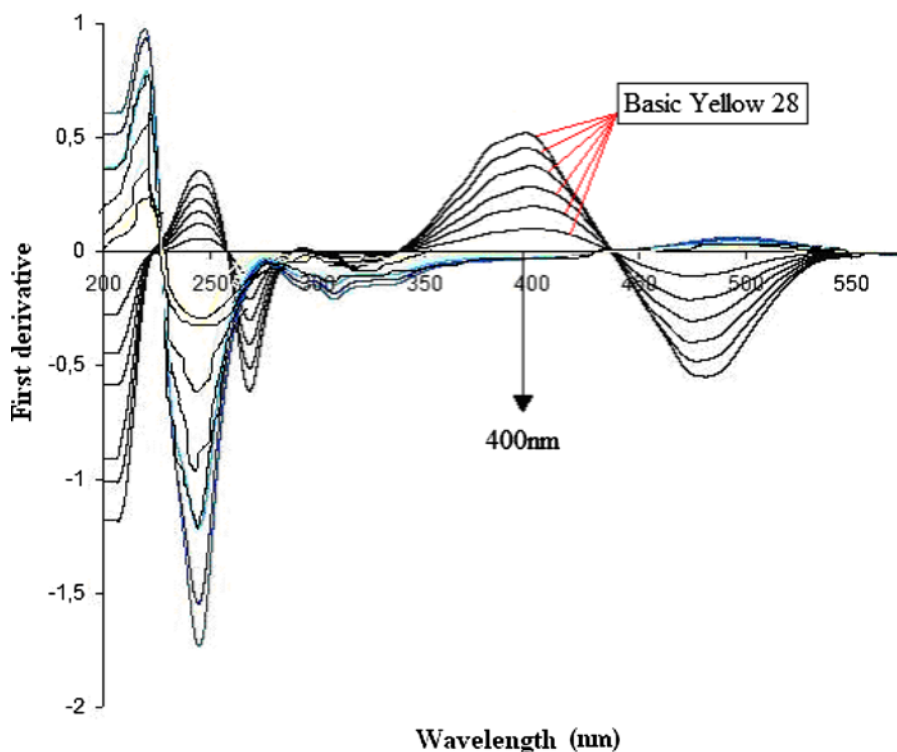


Fig. 3. First derivative spectra of DB56 and BY28.

Table 2
Statistical results of calibration graphs obtained by first derivative method

Method			Regression equation	r	SE(m)	SE(n)	$S(r)$
Derivative	DB56	559	$A = 0.3079C_{DB56} + 0.0,027$	0.9,991	0.0,045	0.0,026	0.0,028
	AV 90	400	$A = 19.058C_{BY28} + 0.0,642$	0.9,937	0.0,297	0.0,116	0.0,124

the aqueous stream as a gelatinous suspension, which can remove the waste matter from wastewater either by complexation or by electrostatic attraction followed by coagulation. Ferric ions electrogenerated may form monomeric ions, ferric hydroxo complexes with hydroxide ions and polymeric species, namely $Fe(H_2O)_6^{3+}$, $Fe(H_2O)_5OH^{2+}$, $Fe(H_2O)_4(OH)_2^+$, $Fe_2(H_2O)_8(OH)_2^{4+}$, $Fe_2(H_2O)_6(OH)_4^{2+}$, and $Fe(OH)_4^-$ depending on the pH range [20].

Disperse dyes are often of anthraquinone and sulfide structures. The disperse dyes are negatively charged in solution. DB56 is an anionic dye [40]. Basic yellow 28, when ionized in aqueous solution, carries a positive charge and is named as a cationic dye [41].

The variation of dye uptake with pH can be explained by considering the difference in the struc-

ture of dyes and the electrokinetic behavior of ferric hydroxide. The ζ -potentials of ferric hydroxide as a function of pH are shown in Fig. 5. It was found that the isoelectric point (IEP) occurred at pH 8 [42]. Increasing pH of the solution causes zeta potential to become increasingly negative up to pH 12. Apparently, the higher the solution pH value, the more the negative charges on the ferric hydroxide surface, the more attractive to cations but not attractive to anions.

At lower pH, a significantly higher electrostatic attraction exists between the positively charged adsorption sites on ferric hydroxide and the negatively charged dyes, thereby causing the increase in anionic DB56 adsorption but the decrease in cationic BY28.

Table 3
Recoveries of DB56 and BY28 in various mixtures by first derivative method

No.	Method Added		Derivative	
	DB56	BY28	559 nm	400 nm
			DB56	BY28
1	6	6	97.2	98.3
2	5	5	98.0	99.6
3	4	4	97.4	97.1
4	5	5	99.2	101.9
5	6	5	98.6	99.6
6	4	3	97.9	98.8
7	5	3	97.5	99.4
8	3	6	99.8	99.3
9	6	3	102.3	97.3
10	5	4	97.8	102.3
11	3	4	101.3	98.3
12	3	5	100.9	99.4
		Mean:	99.0	99.3
		SD	1.72	1.51
		RSD	1.73	1.52

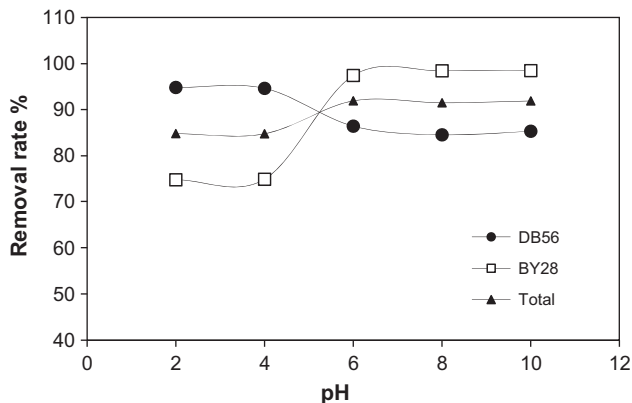


Fig. 4. Effect of initial pH on the removal efficiency of dyes ($t = 10$ min; $C_0 = 100 \text{ mg L}^{-1}$; $i = 10.89 \text{ mA cm}^{-2}$; $T = 293.15 \text{ K}$; $\text{NaCl} = 3 \text{ g L}^{-1}$; $d = 2.2 \text{ cm}$; and agitation speed = 120 rpm).

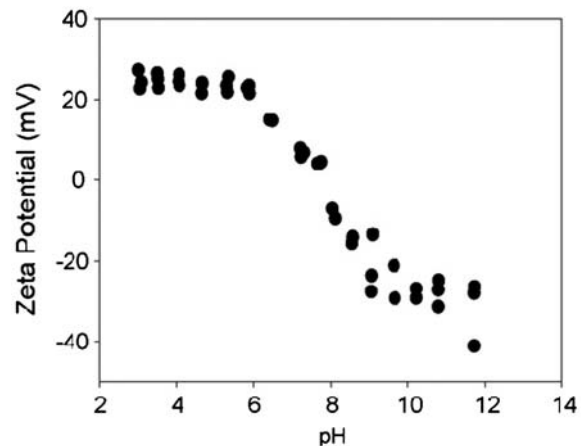
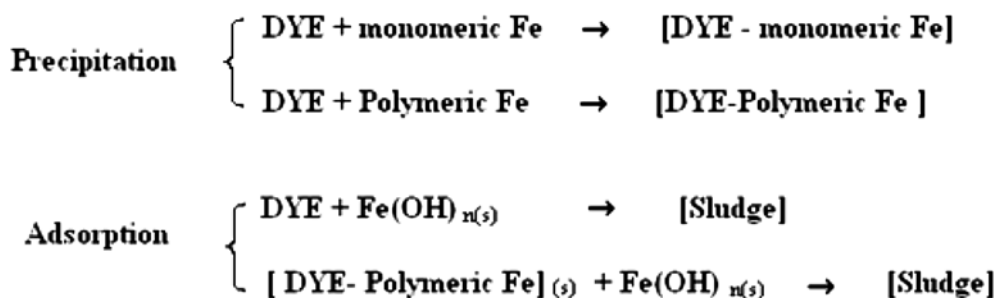


Fig. 5. Zeta potential of ferric hydroxide as a function of pH using 0.01 M NaNO_3 as the supporting electrolyte [42].

As the pH of the system increases, ferric hydroxide appears negatively charged, which does not favor the adsorption of anionic dye molecules due to the electrostatic repulsion between the negatively charged surface and the dye anions. Thus, at higher pH, the uptake of positively charged BY28 would be high, but the uptake of negatively charged DB56 would be low (Fig. 4). At the same time, the presence of excess OH^- ions in alkaline pH will compete with DB56 anions for the adsorption sites.

Mechanism of electrochemical process in aqueous systems is quite complex. However, the color removal process may involve the dye molecule being adsorbed by both electrostatic attraction and physical entrapment. The insoluble metal hydroxides of iron can remove the dye molecules by surface complexation or by electrostatic attraction. In surface complexation, it is assumed that the dye molecule can act as a ligand to bind a hydrous iron moiety with precipitation and adsorption mechanisms [20]:



3.2. Effect of the conductivity

In general, NaCl is used to obtain conductivity in an EC process. Solution conductivity affects current efficiency, cell voltage, and consumption of electrical energy in electrolytic cells. Increasing water conductivity using NaCl also has other advantages: e.g. chloride anions could significantly reduce the adverse effects of other anions on coagulation, such as sulfate or bicarbonate anions.

The effect of conductivity on dye removal was investigated by the addition of NaCl in different amounts. The effect of NaCl concentration on the removal efficiency and the energy consumption is shown in Fig. 6 for the mixture of dyes. The conductivity of the solution and the current density increase when concentration of the salt in solution increases.

The higher ionic strength will generally cause an increase in current density at the same cell voltage or, equivalently, the cell voltage decreases with increasing wastewater conductivity at constant current density. Consequently, the necessary voltage to attain a certain current density will be diminished and the consumed electrical energy will decrease [43]. Although electrolyte concentration helps to increase the conductivity, the results show that color removal efficiency of EC did not change considerably for both dyes in water. According to the results, high color removal percentage with low cell voltages and low energy consumption can be obtained in dye solutions with NaCl of around 3 g L⁻¹. The removal percentages at pH 7 are 86.5% for DB56 and 99.9% for BY28 in the solutions with NaCl of 3 g L⁻¹.

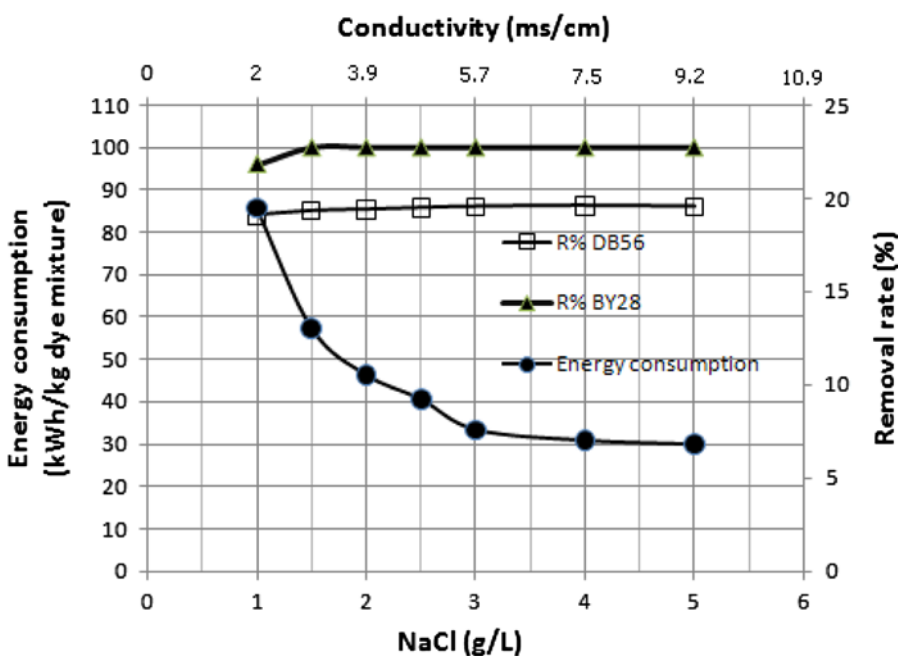


Fig. 6. Effect of conductivity on the energy consumption and the removal efficiency of DB56 and BY28 ($i = 10.89 \text{ mA cm}^{-2}$; $\text{pH} = 7$; $t = 10 \text{ min}$; $C_{0, \text{DB56}} = 100 \text{ mg L}^{-1}$; $C_{0, \text{BY28}} = 100 \text{ mg L}^{-1}$; $T = 298 \text{ K}$; $d = 2.2 \text{ cm}$; and agitation speed = 120 rpm).

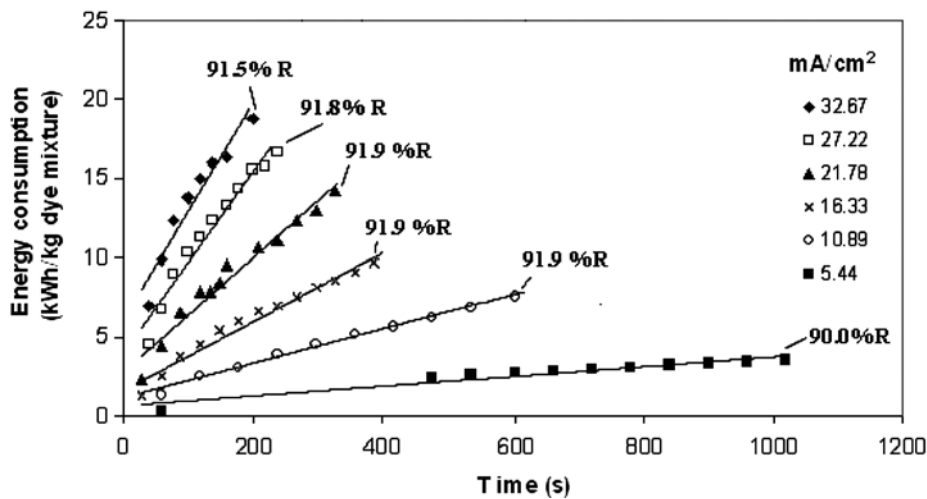


Fig. 7. Effect of electrolysis time and current density on the total removal efficiency of dye mixtures (pH=7; $t = 10$ min; $C_{0,DB56} = 100 \text{ mg L}^{-1}$; $C_{0,BY28} = 100 \text{ mg L}^{-1}$; $T = 298 \text{ K}$; $d = 2.2 \text{ cm}$; and agitation speed = 120 rpm).

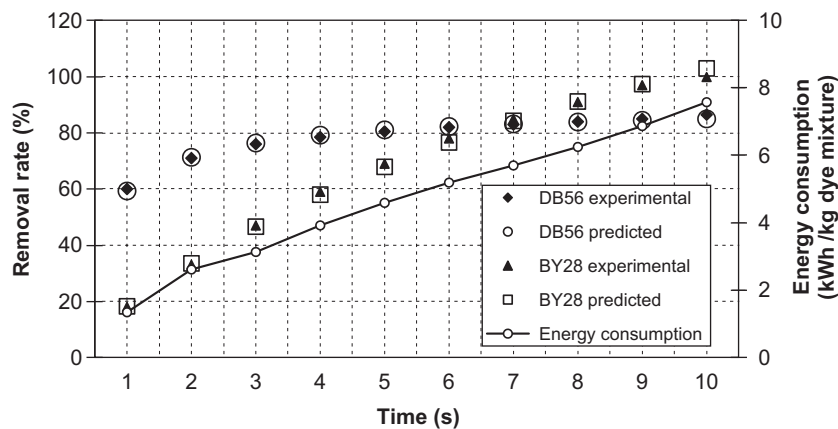


Fig. 8. Effect of electrolysis time on the removal efficiency of DB56 and BY28 (pH=7; $i = 10.89 \text{ mA cm}^{-2}$; $C_{0,DB56} = 100 \text{ mg L}^{-1}$; $C_{0,BY28} = 100 \text{ mg L}^{-1}$; $T = 298 \text{ K}$; $d = 2.2 \text{ cm}$; and agitation speed = 120 rpm).

3.3. Effect of current density and electrolysis time

It is well known that the amount of current density determines the coagulant production rate, and adjusts the rate and size of bubble production, and hence affects the growth of flocs [43]. The effect of current density on the efficiency of color removal was investigated by carrying out the experiments at different current densities. Electrical energy consumption and current efficiency are very important economical parameters in the EC process. Electrical energy consumption was calculated using equation [2]:

$$E = U \cdot I \cdot t_{EC} \quad (3)$$

where E is the electrical energy in Wh, U is the cell voltage in volt (V), I is the current in ampere (A), and t_{EC} is the time of EC process per hour. Figs. 7 and 8 show the effect of current density, electrolysis time, and energy consumption for the simultaneous removal of both dyes in water. In the case of shorter time period and higher current densities, the total removal efficiency did not show too much difference. As shown from Figs. 6 and 7, the optimum energy consumption was observed at 10.89 mA cm^{-2} current density for 10 min of electrolysis time. As shown from Fig. 7, the minimum energy consumption was $7.58 \text{ kWh}(\text{kg dye mixture})^{-1}$ at 10.89 mA cm^{-2} current density for 10 min of electrolysis time.

Table 4
Characteristics parameters calculated for the EC process in optimized conditions^a

Dye	E , kWh (kg dye mixture) ⁻¹	ϕ	SEEC, kWh (kg Fe) ⁻¹
(DB56 + BY28) ^b	7.58	0.85	10.02 ^c

^aNaCl: 3 g L⁻¹; pH=7; electrolysis time: 10 min; current density: 10.89 mA cm⁻²; $C_{0,DB56} = 100$ mg L⁻¹; $C_{0,BY28} = 100$ mg L⁻¹; $T = 298$ K; $d = 2.2$ cm; and agitation speed = 120 rpm.

^bDB56 = 100 mg L⁻¹, and BY28 = 100 mg L⁻¹.

^c $U = 8.9$ V.

The current efficiency (ϕ) of EC process was calculated by Eq. (3). This calculation was based on the comparison of experimental weight loss of iron electrodes (Δm_{exp}) during the EC process with a theoretical amount of iron dissolution (Δm_{theo}) according to Faraday's law [34]:

$$\phi = \Delta m_{exp} / \Delta m_{theo} \tag{4}$$

The specific electrical energy consumption (SEEC) was calculated as a function of iron electrodes' weight consumption during EC in kWh(kgFe)⁻¹ using Eq. (4) [2]:

$$SEEC = (nFU) / (3.6 \cdot 10^3 M \phi) \tag{5}$$

where M is the molar mass of the iron, (g mol⁻¹), n is the number of electron moles, and F is the Faraday constant ($F = 96487$ C mol⁻¹). These calculations were carried out after optimizing the operational parameters in the EC process. The calculated values are shown in Table 4.

The total iron dissolution found from experimentations is about 15% lower than that predicted from Faraday's law.

A simple model can be used to demonstrate the relationship between dye concentration removed and residual dye concentration [21]. We have found previously that there is a linear relationship between the dye concentration removed per mass of dissolved iron during electrolysis and the residual dye concentration:

$$\Delta R / m_{Fe} = k + l C_{res} \tag{6}$$

Table 5
 k and l constants for DB56 and BY28

	k	l	R^2
DB56	-631.12	58.628	0.99
BY28	312	2.742	0.98

where ΔR is the dye concentration (mg L⁻¹) removed from wastewater, m_{Fe} is the mass of dissolved iron during the electrolysis (g/L), C_{res} is the residual mass concentration of the dyes (mg L⁻¹), the coefficient k denotes the dye removal capacity (mg dye per g iron), and l is another coefficient (L/g iron). m_{Fe} was calculated from Faraday's law.

$$m_{Fe} = \frac{56 \cdot I \cdot t_{EC}}{2.96, 500} \tag{7}$$

The values of k and l were calculated from the slope and intercept of the linear plot, $\Delta R / m_{Fe}$ vs. C_{res} , and are represented in Table 5.

A relationship between Eqs. (6) and (7) can be derived as:

$$m_{Fe} = \frac{\Delta R}{l \cdot C_{res} + k} = \frac{56 \cdot I \cdot t_{EC}}{2.96, 500} \tag{8}$$

The residual mass concentration of the dye (mg L⁻¹) may be given by

$$C_{res} = C_0 - \Delta R \tag{9}$$

where C_0 is the initial mass concentration of the dyes (mg L⁻¹), I is the electric current (Ampere), and t_{EC} is time (s).

If Eq. (9) is substituted into Eq. (8):

$$\Delta R = [l(C_0 - \Delta R) + k] \cdot I \cdot t_{EC} (2.9 \cdot 10^{-4}) \tag{10}$$

Then,

$$\begin{aligned} &\Delta R (1 + l \cdot I \cdot t_{EC} \cdot 2.90 \cdot 10^{-4}) \\ &= l \cdot C_0 \cdot I \cdot t_{EC} \cdot 2.90 \cdot 10^{-4} + k \cdot I \cdot t_{EC} \cdot 2.90 \\ &\cdot 10^{-4} \end{aligned} \tag{11}$$

Taking into account Eq. (4)

$$A = I \cdot t_{EC} \cdot \phi \cdot 2.90 \cdot 10^{-4} \tag{12}$$

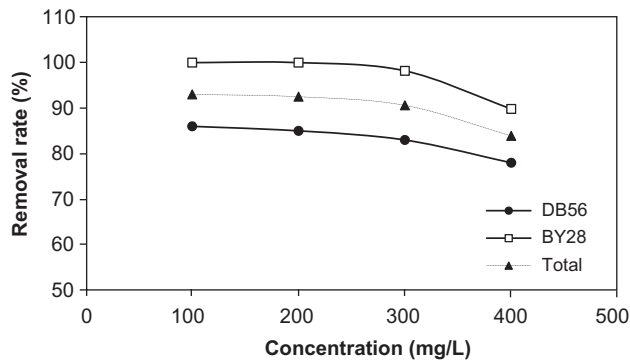


Fig. 9. Effect of initial concentration on the removal efficiency of DB56 and BY28 (pH=7; $i=10.89 \text{ mA cm}^{-2}$; $t=10 \text{ min}$; $T=298 \text{ K}$; $d=2.2 \text{ cm}$; and agitation speed = 120 rpm).

The dye concentration (mg L^{-1}) removed from the wastewater is then estimated to be

$$\Delta R = \frac{A(k + I \cdot C_0)}{1 + I \cdot A} \quad (13)$$

where C_0 is the initial mass concentration of the dyes (mg L^{-1}), I is the electric current (Ampere), and t_{EC} is time (s).

The predicted ΔR values for various t values were calculated using Eq. (6). Fig. 7 shows a comparison between the predicted values and the experimental data. As can be seen in Fig. 7, the calculated values were found to generate a satisfactory fit to the experimental data.

3.4. Effect of the initial concentration

A series of batch experiments with initial dye concentrations at constant current density were performed to derive the influence of initial concentrations on dye removal. Fig. 9 shows the effect of initial dye concentrations on removal efficiencies of both dyes. As it is expected, at low concentration ranges, the removal efficiency was higher than the high initial dye concentrations. The removal percentages were 86.2–78.3% for DB56, 99.9–89.8% for BY28, and 93–83.9% for total removal in the concentration range of 100 to 400 ppm in 10 min. The required amounts of coagulant produced electrochemically for the dye removal are increased with the increase of dyestuff concentration. Our experiments were all performed under the same operating conditions, the release rate of the hydroxyl radicals being almost constant. Therefore, under the present experimental conditions, the lower initial dyestuff concentration yields a better

color removal efficiency. An increase in the dyestuff concentration caused a decrease in the removal rate.

4. Conclusions

EC has been evaluated as a tool for DB56 and BY28 dyes from aqueous solutions in an EC reactor with iron electrodes. The effect of various operational parameters on color removal efficiency was investigated and optimized. The simultaneous removal of both dyes was found to be affected by the initial pH of the solution, electrolysis time, initial dye concentration, current density, and electrolyte concentration. The color removal efficiencies for DB56 and BY28 were 86.2 and 99.9%, respectively, under the conditions of initial pH of 7, initial concentration 100 mg L^{-1} , current density 10.89 mA cm^{-2} , concentration of salt $3,000 \text{ mg L}^{-1}$, and distance between the electrodes 2.2 cm . It was found that the proper electrolysis time for the removal of color from this dye solution was 10 min. The color removal efficiency by EC decreased when the initial dye concentration was more than 200 mg. At above optimal conditions, the power requirement and SEEC were $7.58 \text{ kWh (kg dye)}^{-1}$ mixture and $4.37 \text{ kWh (kg Fe)}^{-1}$, respectively. The apparent current efficiency for the dye mixture was about 85%. The dye removal efficiencies for the various electrolysis times from an equation developed were calculated. The results showed that this model was found to be in good agreement with the experimental results. The process of bringing down the dye concentrations levels of waste below the acceptable values before discharging into surface water sources is studied in detail in the present work and this method can be used for the removal of dye mixtures from the wastewaters.

Symbols

C_0	— concentrations of dye before, mg L^{-1}
C	— concentrations of dye after electrocoagulation, mg L^{-1}
CR (%)	— color removal efficiency
RSD	— relative standard deviation
SD	— standard deviation
\bar{x}	— the average result
E	— electrical energy, Wh
EC	— electrocoagulation
DC	— direct current
U	— cell voltage in volt
I	— current in ampere
t_{EC}	— time of EC process, h
ϕ	— current efficiency

Δm_{exp}	— experimental weight loss of iron electrodes, g
Δm_{theo}	— theoretical amount of iron dissolution, g
SEEC	— specific electrical energy consumption, kWh (kg Fe) ⁻¹
F	— Faraday constant
n	— number of electron moles
M	— molar mass of the iron
ΔR	— dye concentration (mg L ⁻¹) removed
m_{Fe}	— mass of dissolved iron, g L ⁻¹
C_{res}	— residual mass concentration of the dyes, mg L ⁻¹
k	— dye removal capacity, mg dye per g iron
l	— isotherm coefficient, L/g iron

References

- Cañizares, F. Martínez, C. Jiménez, J. Lobato, M.A. Rodrigo, Coagulation and electrocoagulation of wastes polluted with dyes, *Environ. Sci. Technol.* 40 (2006) 6418–6424.
- Daneshvar, A. Oladegaragoze, N. Djafarzadeh, Decolorization of basic dye solutions by electrocoagulation: An investigation of the effect of operational parameters, *J. Hazard. Mater. B* 129 (2006) 116–122.
- Daneshvar, H. Ashassi-Sorkhabi, A. Tizpar, Decolorization of orange II by electrocoagulation method, *Sep. Purif. Technol.* 31 (2003) 153–162.
- Ozdemir, B. Armagan, M. Turan, M.S. Celik, Comparison of the adsorption characteristics of azo-reactive dyes on mesoporous minerals, *Dyes Pigments* 62 (2004) 49–60.
- Q. Liu, Y. Zhou, L. Zou, T. Deng, J. Zhang, Y. Sun, X. Ruan, P. Zhu, G. Qian, Simultaneous wastewater decoloration and fly ash dechlorination during the dye wastewater treatment by municipal solid waste incineration fly ash, *Desalin. Water Treat.* 32 (2011) 179–186.
- Z. Wanga, P. Hanb, Y. Jiaob, D. Mab, C. Doub, R. Han, Adsorption of congo red using ethylenediamine modified wheat straw, *Desalin. Water Treat.* 30 (2011) 195–206.
- E. Bulut, M. Ozacar, I.A. Sengil, Equilibrium and kinetic data and process design for adsorption of Congo Red onto bentonite, *J. Hazard. Mater.* 154 (2008) 613–622.
- M. Ozacar, I.A. Sengil, A two stage batch adsorber design for methylene blue removal to minimize contact time, *J. Environ. Manage.* 80 (2006) 372–379.
- M.X. Zhu, L. Lee, H.H. Wang, Z. Wang, Removal of an anionic dye by adsorption/precipitation processes using alkaline white mud, *J. Hazard. Mater.* 149 (2007) 735–741.
- Gatut Sudarjanto., Beatrice Keller-Lehmann, Jurg Keller, Optimization of integrated chemical-biological degradation of a reactive azo dye using response surface methodology, *J. Hazard. Mater. B* 138 (2006) 160–168.
- A.R. Khataee, M.B. Kasiri, Photocatalytic degradation of organic dyes in the presence of nanostructured titanium dioxide: Influence of the chemical structure of dyes, *J. Mol. Catal. A: Chem.* 328 (2010) 8–26.
- Jinwook Chunga., Jong-Oh Kim, Application of advanced oxidation processes to remove refractory compounds from dye wastewater, *Desalin. Water Treat.* 25 (2011) 233–240.
- M.A.M. Martins, I.C. Ferreira, I.M. Santos, M.J. Queiroz, N. Lima, Biodegradation of bioaccessible textile azo dyes by *Phanerochaete chrysosporium*, *J. Biotechnol.* 89 (2001) 91–98.
- M.A. Mazmanci, A. Ünyayar, Decolourisation of Reactive Black 5 by *Funalia trogii* immobilised on *Luffa cylindrica* sponge, *Process Biochem.* 40 (2005) 337–342.
- B. Shi, G. Li, D. Wang, C. Feng, H. Tang, Removal of direct dyes by coagulation: The performance of preformed polymeric aluminum species, *J. Hazard. Mater.* 143 (2007) 567–574.
- E. Guibal, J. Roussy, Coagulation and flocculation of dye-containing solutions using a biopolymer (Chitosan), *React. Funct. Polym.* 67 (2007) 33–42.
- T.H. Kim, C. Park, J. Yang, S. Kim, Comparison of disperse and reactive dye removals by chemical coagulation and Fenton oxidation, *J. Hazard. Mater. B* 112 (2004) 95–103.
- F.R. Furlan, L.G.M. deSilva, A.F. Morgado, A.A.U. de Souza, S.M.A.G.U. de Souza, Removal of reactive dyes from aqueous solutions using combined coagulation/flocculation and adsorption on activated carbon, *Resour. Conserv. Recy.* 54 (2010) 283–290.
- M. Riera-Torres, C. Gutiérrez-Bouzán, M. Crespi, Combination of coagulation-flocculation and nanofiltration techniques for dye removal and water reuse in textile effluents, *Desalination* 252 (2010) 53–59.
- İ.A. Sengil, M. Ozacar, The decolorization of C.I. Reactive Black 5 in aqueous solution by electrocoagulation using sacrificial iron electrodes, *J. Hazard. Mater.* 161 (2009) 1369–1376.
- İ.A. Şengil, M. Özacar, B. Ömürlü, Decolorization of C.I. reactive red 124 using the electrocoagulation method, *Chem. Biochem. Eng. Q* 18 (2004) 391–401.
- A.K. Golder, N. Hridaya, A.N. Samanta, S. Ray, Electrocoagulation of methylene blue and eosin yellowish using mild steel electrodes, *J. Hazard. Mater. B* 127 (2005) 134–140.
- C. Phalakornkule, S. Polgumhang, W. Tongdaung, B. Karakat, T. Nuyut, Electrocoagulation of blue reactive, red disperse and mixed dyes, and application in treating textile effluent, *J. Environ. Manage.* 91 (2010) 918–926.
- E.-S.Z. El-Ashtoukhy, N.K. Amin, Removal of acid green dye 50 from wastewater by anodic oxidation and electrocoagulation—a comparative study, *J. Hazard. Mater.* 179 (2010) 113–119.
- F. Zidane, P. Droguin, B. Lekhlif, J. Bensaïd, J. Blais, S. Belcadi, K. El kacemi, Decolourization of dye-containing effluent using mineral coagulants produced by electrocoagulation, *J. Hazard. Mater. B* 155 (2008) 153–163.
- A. Aleboye, N. Daneshvar, M.B. Kasiri, Optimization of C.I. acid red 14 azo dye removal by electrocoagulation batch process with response surface methodology, *Chem. Eng. Process* 47 (2008) 827–832.
- N. Daneshvar, H.A. Sorkhabi, M.B. Kasiri, Decolorization of dye solution containing Acid Red 14 by electrocoagulation with a comparative investigation of different electrode connections, *J. Hazard. Mater. B* 112 (2004) 55–62.
- Y.A. Xiong, P.J. Strunk, H. Xia, X. Zhu, H.T. Karlsson, Treatment of dye wastewater containing acid orange II using a cell with three-phase three-dimensional electrode, *Water Res.* 35 (2001) 4226–4230.
- Y.S. Yildiz, Optimization of bomaplex Red CR-L dye removal from aqueous solution by electrocoagulation using aluminum electrodes, *J. Hazard. Mater.* 153 (2008) 194–200.
- M.Y.A. Mollah, S.R. Pathak, P.K. Patil, M. Vayuvegula, T.S. Agrawal, J.A.G. Gomes, M. Kesmez, D.L. Cocke, Treatment of orange II azo-dye by electrocoagulation (EC) technique in a continuous flowcell using sacrificial iron electrodes, *J. Hazard. Mater. B* 109 (2004) 165–171.
- M. Kobya, E. Demirbas, O.T. Can, M. Bayramoglu, Treatment of levafix orange textile dye solution by electrocoagulation, *J. Hazard. Mater. B* 132 (2006) 183–188.
- E.-S.Z. El-Ashtoukhy, N.K. Amin, Removal of acid green dye 50 from wastewater by anodic oxidation and electrocoagulation—a comparative study, *J. Hazard. Mater.* 179 (2010) 113–119.

- [33] S. Aoudj, A. Khelifa, N. Drouiche, M. Hecinia, H. Hamitouche, Electrocoagulation process applied to wastewater containing dyes from textile industry, *Chem. Eng. Process.* 49 (2010) 1176–1182.
- [34] A.R. Khataee, V. Vatanpour, A.R.A. Ghadim, Decolorization of C.I. Acid Blue 9 solution by UV/Nano-TiO₂, Fenton, Fenton-like electro-Fenton and electrocoagulation processes: A comparative study, *J. Hazard. Mater.* 161 (2009) 1225–1233.
- [35] C. Phalakornkule, P. Sukkasem, C. Mutchimsattha, Hydrogen recovery from the electrocoagulation treatment of dye-containing wastewater, *Int. J. Hydrogen Energ.* 35 (2010) 10934–10943.
- [36] T.H. Kim, C. Park, E.B. Shin, S. Kim, Decolorization of disperse and reactive dyes by continuous electrocoagulation process, *Desalination* 150 (2002) 165–175.
- [37] I. Kabdaslı, B. Vardar, I. Arslan-Alaton, O. Tünay, Effect of dye auxiliaries on color and COD removal from simulated reactive dyebath effluent by electrocoagulation, *Chem. Eng. J.* 148 (2009) 89–96.
- [38] W. Balla, A.H. Essadkia, B. Gouricha, A. Dassaab, H. Chenika, M. Azzi, Electrocoagulation/electroflotation of reactive, disperse and mixture dyes in an external-loop airlift reactor, *J. Hazard. Mater.* 184 (2010) 710–716.
- [39] R. Kramer, *Quantification Chemometric Techniques for Quantitative Analysis*, Marcel Dekker, New York, NY, 1998.
- [40] Y. Chen, Zh.Y. Zhang, Zh.H. Zhu, A study of the influences of inorganic electrolyte on the stability and the electrokinetic properties of the aqueous dispersions of organic dye, *J. Chem. Ind. Eng.* 5 (1989) 613–618.
- [41] A. Olgun, N. Atar, Equilibrium and kinetic adsorption study of Basic Yellow 28 and Basic Red 46 by a boron industry waste, *J. Hazard. Mater.* 161 (2009) 148–156.
- [42] X.H. Guan, J. Wang, C.C. Chusuei, Removal of arsenic from water using granular ferric hydroxide: Macroscopic and microscopic studies, *J. Hazard. Mater.* 156 (2008) 178–185.
- [43] M.Y.A. Mollah, R. Schennach, J.R. Parga, D.L. Cocke, Electrocoagulation (EC)-science and applications, *J. Hazard. Mater. B* 84 (2001) 29–41.